Automated PCB Inspection System

Syed Usama BUKHARI [1], Ioan BONDREA [2], Remus BRAD [2]

[1]Department of Computer Science, COMSATS IIT, ChakShazad, 44000, Islamabad, Pakistan
[2] Faculty of Engineering, Lucian Blaga University of Sibiu, Sibiu, 550024, Romania

***Abstract* – Development of an automated PCB inspection system as per the need of industry is a challenging task. In this paper a case study is presented, to exhibit, a proposed system for an immigration process of a manual PCB inspection system to an automated PCB inspection system, with a minimal intervention on the existing production flow, for a leading automotive manufacturing company. A detailed design of the system, based on computer vision followed by testing and analysis was proposed, in order to aid the manufacturer in the process of automation.**

***Keywords* – Printed Circuit Board, Automated Visual Inspection, Computer Vision, Quality Assurance.**

1. Introduction

Bruce G. and Paul F. presented two case studies in their book [1], in order to illustrate the complexity of designing and building an industrial vision system. The authors emphasized how design of a vision system became simplified, if a detailed knowledge of the application is known. They also claim that, developing a reasonable industrial vision system is virtually impossible if the system does not have control over external devices, such as lamps, cameras, lenses, robots etc.

The product Quality Assurance (QA) is an important feature also in terms of building the customer's confidence. A QA system, which insures 0% defects is on the goals of every company, and in order to be achieved, a lot of resources and time is allocated to the inspection process, at different stages of manufacturing. The human inspection was considered the best inspection option, due to the versatility, not only based upon some guidelines, but also analytically and subjectively. However, the drawback of human inspection is its speed, the difference in skills and the potential of long working hours. In this paper, the developing of a quality assurance system using computer vision is present.

The paper is structured as follows; section II gives a brief literature review, followed by the presentation of the current PCB inspection, in section III. The proposed system is presented in section IV, while the obtained results are in section V followed by conclusions and future work directions in section VI.

DOI: 10.18421/TEM62-25
https://dx.doi.org/10.18421/TEM62-25

Corresponding author: Syed Usama BUKHARI,
Department of Computer Science, COMSATS IIT, Islamabad, Pakistan
Email: syedusama@gmail.com

2. Automatic Visual Inspection Systems

The PCB inspection process can be divided into two main classes: electrical / contact methods and not electrical / non-contact methods [6]. The first category methods are reliable in inspecting the design parameters and manage to detect the connectivity of the circuit, still having their limitations. Cosmetic errors, the check of track widths or spacing/insulation issues, are few examples where electrical inspection method fails to perform [15]. The non-contact methods currently used in the industry are: Automatic Visual Inspection (AVI), X-ray Imaging, Scanned Beam Lamniography, Ultrasonic Imaging, Thermal Imaging and Laser Scanning [6], [15]. A complete summary of major issues involved in PCB inspection can be found in [7], [14], [16], [17].

The major PCB manufacturing stages are: bare-board fabrication, loaded board assembly and the soldering process [6]. The problems with loaded-board and soldered-board inspection have been addressed, but the results are typically limited to the detection of most noticeable discrepancies only [8]. In [9], Ajay argues that in order to reduce the defects, the PCB inspection should be at least completed in the three main steps of the manufacture: PCB printing, components assembly on the PCB surface and soldering. In the late 1980s and early 1990s, a number of researchers started presenting the possible drawbacks of using human inspection [10], [11], [12], [13]:

- Manual inspection is slow, costly and leads to excessive scrap rates and finally does not assure high quality;
- Multi-layer boards are not suitable for human inspection;
- With the aid of magnification mechanism, human workers are able to detect faults at high rate, though in multi-layer boards the average is close to 50%. Latest digital image processing helps improving the average, but requires even more time;
- At the current quality level requirement in the industry, sampling inspection is not applicable.

The main drawback of AVI systems is their need to be customized for every problem, which made them only suitable for one specific application [22].

The PCBs are inspected extensively; this inspection starts before the assembly of any components or the soldering process and still, bare board defects exist. Hall [17] provides the outline of the processing and post-processing steps required for the verification of artwork design. The types of defects on a single layer PCB are: Breakout, Pin-hole, Open Circuit, Under-etch, Mouse-bite, Missing Conductor, Spur, Short, Wrong Size Hole, Conductor too Close, Spurious Copper, Excessive Short, Missing Hole, Over-etch [15]. The Open / Partial Open, Short Pinhole, Breakout, Over-etch, Under-etch are the most frequent defects [6].

In [18], Kumar, Ajay and Pang present a summary of occurring causes of defects during fabrication. Heriansyah et al. [19] used the Vector Quantization Neural Network to classify possible PCB defects, while Lin et al. [20] proposed a two-stage method, in order to classify defects using Neural Networks. Khalid et al. [21], employed a technique which identifies and groups the PCB defects into five classes using binary images. Putera et al. [15] used image processing and segmentation algorithm to improve Khalid's work and classify the defects into seven groups. Londe and Chavan [14] improved Khalid's work from five to fourteen classes.

The PCB defects can be broadly divided into two classes: potential and fatal defects. Potential defects are those defects, which compromise the PCB performance, whereas fatal defects are the ones which make PCB unable to meet its design objectives.

3. Analysis of the current AVI system

To develop a new system, based of the existing working scheme, is very difficult, especially in the case where the alteration of the existing system is required by a leading automotive manufacturing company, specialized in the development of different automotive modules. The DQ 200 TCU control unit PCB examination was requested to be reformed, in terms of time interval necessary for the inspection after the board has passed through the soldering process. The workflow is described in figure 1., showing the whole manufacturing process, while the human inspection was presented in figure 2.

Figure 1. Block diagram of DQ 200 TCU manufacturing process

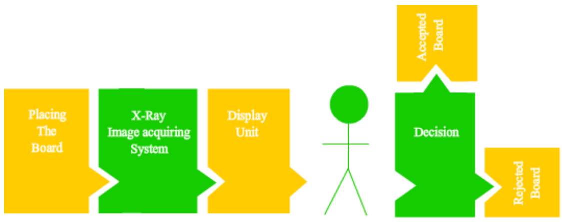

Figure 2. Block diagram of Human Quality Inspection

The procedures of human inspection are:

1. The worker places the board in the image-acquiring unit;
2. Each board is divided into 15 different sections. The sub-image of every section is extracted from an X-ray camera with microscopic lenses and presented to the worker on a display unit;
3. After thoroughly examining every single image, the skilled worker decides if all the sub-images pass the required criteria. Then that board is moved to further operations. However, if any criteria are not matched, then the board is sent back for repairing.

The worker has to check the following in order to reach a conclusion:

- The board should not contain any big soldering joints, which were not part of the original design;
- The soldering joints are well soldered;
- The pins of the circuits do not have any cracks;
- The circuits are not overlapped or too close to each other.

According to the company, the average time to perform this check on every board by a human is approximately two minutes (this includes placing the board in the image-acquiring unit, checking and taking it out of the unit), which is the most time consuming step of the whole chain. The company records shows that, on average, one human worker achieved less than 2 % percent errors. With current system, the total number of boards checked every day is approximately 1200 to 1300 and on average, less than 3% boards have defects. To achieve that output productivity, two parallel inspection lines were established; requiring four skilled workers to perform the desired tasks.

A statistical computation of the time and resources consumed by the existing inspection has been done. The system needed to run 24 hours, split into 3 shifts of 8 hours for workweek days, while on weekends it is split into 4 shifts of 6 hours each. During each shift, a worker is allowed to take two breaks of 5 minutes each and one 30 minutes break for meal. Watching consistently the display and concentrating visually for a long period of time, makes the inspection a difficult job and therefore workers are shifted every 2 hours. This process also wastes a certain amount of time. It is worth mentioning that the training period for a skilled inspector could least for a minimum of 15 days.

Equations 1 and 2 give the generic formula to calculate the wastage of time in one workweek day and one weekend day:

$$t_b = \sum_{i=1}^{n}\left(\sum_{j=1}^{c} t_{b1} + t_{b2} + t_{b3}\right); \quad n = 3 \qquad (1)$$

$$t_{bw} = \sum_{i=1}^{n}\left(\sum_{j=1}^{c} t_{b1} + t_{b2} + t_{b3}\right); \quad n = 4 \qquad (2)$$

where n is the total number of shifts in a day, c is total number of breaks in one shift, t_{b1} is time of a break, t_{b2} is the time of a meal break, t_{b3} is the time used for shifting. Equation 3 gives the total working time of one workweek day, where equation 4 gives the total working time for one weekend day:

$$\Delta t = t_t - t_b \qquad (3)$$

$$\Delta t_w = t_t - t_{bw} \qquad (4)$$

where t_t is total work time. Equation 5 gives the total number of boards that can be checked in one workweek day, while equation 6 gives the total number of boards checked in one weekend day:

$$B_1 = \frac{\Delta t}{t_1} \qquad (5)$$

$$B_2 = \frac{\Delta t_w}{t_1} \qquad (6)$$

where t_1 is the total time required to check one board. Equation 7 gives the total number of boards that can be checked in one week:

$$B_w = \sum_{i=1}^{n} B_1 + \sum_{j=1}^{m} B_2 \qquad (7)$$

The total number of boards in one week, which could be checked in the wasted span of time given by equation 8:

$$B_d = \frac{\sum_{i=1}^{n} t_b + \sum_{j=1}^{m} t_{bw}}{t_1} \qquad (8)$$

In our particular case, t_1 = 120 sec, t_{b1} = 300 sec, t_{b2} = 1800 sec, t_{b3} = 300 sec, t_b = 9900 sec, t_{bw} = 13200 sec, $\Delta\ t$ = 76500 sec, $\Delta\ t_w$ = 73200 seconds and the followings results were obtained. If we accept a 3% of defects, an average cost of 2 $ per board and a cost of 15 days of training (1057800 seconds), then the yearly costs are shown in table 1.

Table 1. Cost estimation for one quality inspection system

	B_w	B_d	Percentage of B_d	Error	Cost of B_d and error
Week	4408	633	14.4 %	132	1529
Month	17630	2530	14.4 %	529	6118
Year	211560	30360	14.4 %	6347	91044

The company is aware of its time and resource losses and the main requirement was a desired average time to perform one inspection operation, on a single board, to be less than 30 seconds.

Figure 3. shows the 15 sub-images taken from the X-ray camera, which are displayed on monitors to the workers in order to identify the errors.

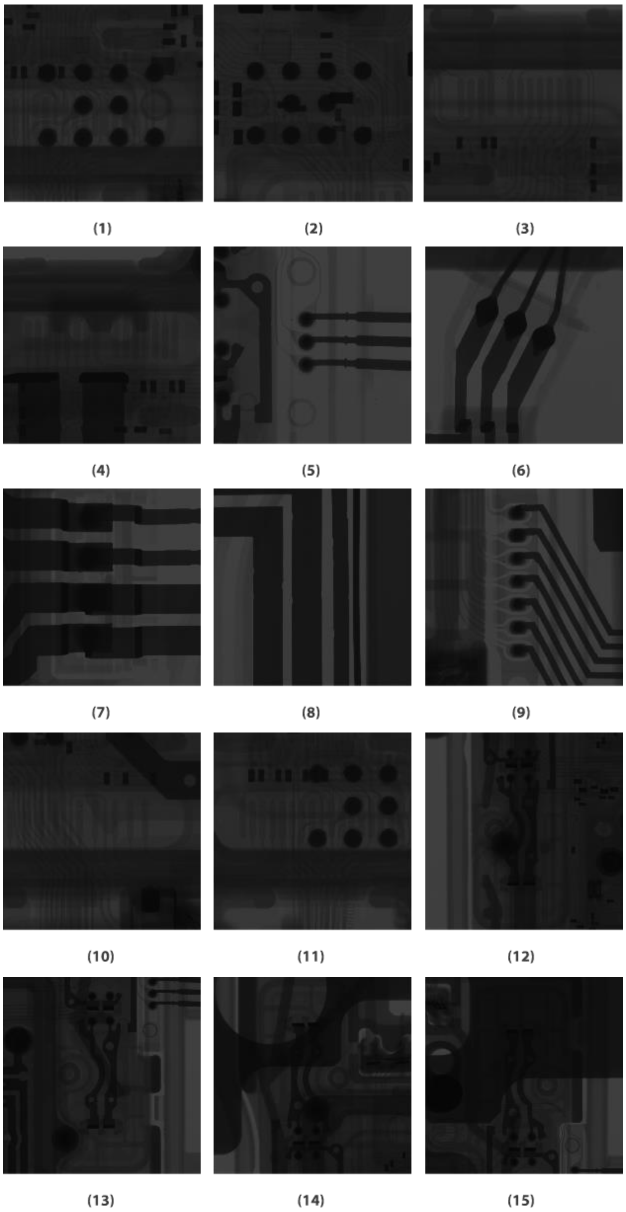

Figure 3. Sub-images of different areas of the PCB

For the images in figure 3.1 and 3.2, the ground truth is also available, which is used to overlap on the acquired images. The overlapping gives three visible outputs to the inspector: 1) the gray level shows the area, which is similar to the ground truth; 2) the white level indicates missing areas in new image, which are present in ground truth; 3) the black regions show the areas, which are not present in the ground truth, but are present in the acquired image. Hence these areas can be noise or soldering balls.

Figure 4. shows overlapping of ground truth of figure 3.1 and 3.2 with the main objective to help the skilled worker making accurate and fast decisions.

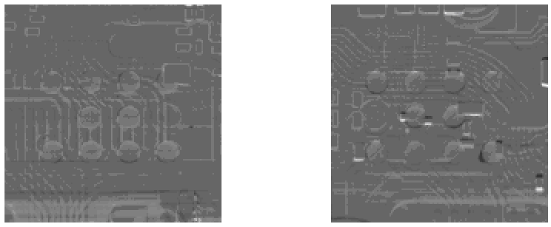

Figure 4. Result of the overlapping of acquired image with ground truth

The aim of our project was to develop a system in order to reduce the inspection time, according to different requirements needed to be fulfilled. Each sub-image contains areas from the board necessary to be tested and with different criteria, as listed below.

Image 3.1 and 3.2:

- Known number of soldering joints should be detected;
- All soldering joints should nearly have equal size;
- All soldering joints should nearly be at the same distance from each other, both vertically and horizontally;
- All soldering joints should be almost dark.

Image 3.3, 3.4, 3.10 and 3.11:

- The thickness of the circuit tracks should nearly be the same;
- Distance between circuit tracks should be sufficient.

Image 3.5, 3.6 and 3.9:

- All circuit tracks should be complete, with no break;
- Known number of soldering joints should be detected;
- All soldering joints should nearly have equal size;
- All soldering joints should nearly be at the same distance from each other, both vertically and horizontally;
- All soldering joints should be almost dark.

Image 3.7:

- All circuit tracks should be complete, with no breaks;
- Distance between circuit tracks should be sufficient.

Image 3.8:

- Distance between circuit tracks should be sufficient.

Also, all the tested sub-images are checked for unwanted soldering balls.

The biggest limitation was that no changes in the current infrastructure have to be made. This issue led to a number of complications. Nevertheless, in the above requirements there are number of terms, which can be viewed as fuzzy, as there are no discrete values present that could define the terms like, big soldering ball, appropriate or nearly the same distance between circuit tracks or soldering joints, soldering joints should be almost dark. Currently, the human expert knows what might be right and what might wrong.

The alignment of the images was another issue, as no two images of the same parts from two different boards were aligned respectively to each other. Either the camera or the board was displaced while the pictures where acquired. This made impossible the selection of ground truth images, without extra processing.

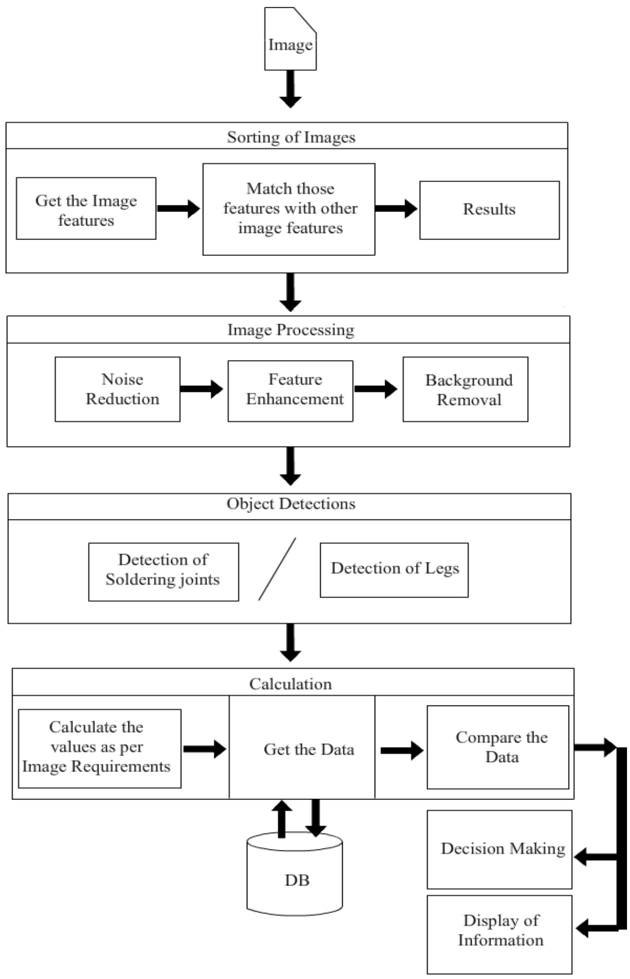

Figure 5. Block diagram of the proposed system

4. The proposed system

The current system is well defined and in use for some time, the only drawback is its dependency on a human skilled worker, having their own limitations due to their nature or capabilities. The main objective of our research was to minimize the inspection time and an automated inspection system was developed. The proposed framework has four main steps: 1) classification of images; 2) image processing; 3) object detection; 4) defect detection. Figure 5. presents the flow diagram of the process.

From figure 5., one can observe how an acquired X-ray image passes through the different steps, as mention above. First, the image is arriving to the classification step, where it will be classified in one of the 15 different known classes. The following step actions are dependent to the given class. Further, the image is passed to image processing step, where noise and background are removed and the image is enhanced for further processing. The enhanced image is then checked for objects like soldering ball, soldering joints and circuit tracks. The last step will compare the already known data with the data from the new image and send the information to the decision-making step.

There are 15 cases to deal with, among them four cases do not have any specific criteria beside the check for unwanted soldering balls. After carefully examining the requirements, the images were divided into 5 groups.

Table 2. Requirements for the image inspection

Requirements List.	
Group 1	• Known number of soldering joints should be detected. • All soldering joints should nearly have equal size. • All soldering joints should nearly be at the same distance from each other, both vertically and horizontally. • All soldering joints should be almost dark. *Group 1 contains image type 3.1 and 3.2*
Group 2	• The thickness of the circuit tracks should nearly be same. • Distance between circuit tracks should be sufficient. *Group 2 contains image type 3.3, 3.4, 3.10 and 3.11*
Group 3	• All circuit tracks should be complete; there should be no break in them. • Known number of soldering joints should be detected. • All soldering joints should nearly have equal size. • All soldering joints should nearly be at the same distance from each other, both vertically and horizontally.

	• All soldering joints should be almost dark. *Group 3 contains image type 3.5,3.6 and 3.9*
Group 4	• All circuit tracks should be complete; there should be no breaks in them. • Distance between circuit tracks should be sufficient. *Group 4 contains image type 3.7*
Group 5	• Distance between circuit tracks should be sufficient. *Group 5 contains image type3.8*

To perform the inspection operations and fulfill all the criteria, a number of different techniques will be used. Therefore, the goal was to use the techniques and algorithms for majority of cases, as no processing time will be wasted.

In the first step, the image is classified using a histogram-based algorithm. After the classification, a Hough circle detection algorithm [2] was applied in order to find any soldering balls. If no shape is found, then the sub-image is considered as without defect and it passes to the next step. In the other case, the system considers the detected shapes as undesired soldering balls. The detected soldering balls are then compared with a threshold size values. The soldering balls remaining under the threshold are ignored, while the soldering balls above the threshold make the board rejection.

The threshold value has been extracted using a set of true positive test images provided by the company. Examining the images, a number of different sized soldering balls were detected and a threshold was set, based upon their size.

4.1. Detection of group 1 type of defects

In order to check group 1 types of sub-images, the following processing has to be completed: 1) image enhancement; 2) finding the soldering joints; 3) computing the size of detected soldering joint; 4) calculate the distance, both horizontally and vertically, between neighboring soldering joints; 5) check the gray level of the soldering joints.

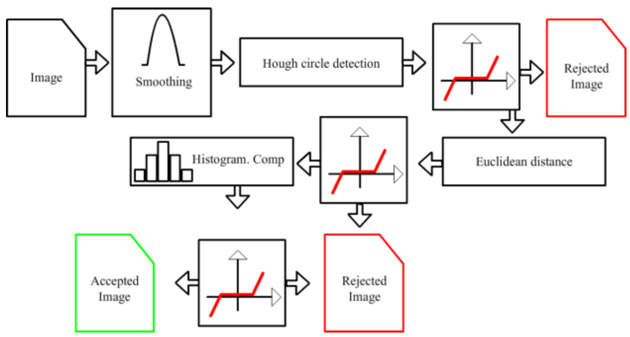

Figure 6. Block diagram of group 1 checking process

A Gaussian filter [3] was applied for the enhancement of images, having a 3x3 kernel and a sigma value equal to 0.5. The detection of soldering joints is performed using a Hough circle detector [3]. Using a minimum and a maximum radius values, extracted empirically form of the set of test image, the algorithm was speeded-up in the identification of soldering joints. At the end, the following information is being retrieved: 1) number of circles in the image; 2) the center of the detected circles; 3) the radius of all the detected circles.

If the number of soldering joints is known, together with their positions and radiuses, the system will reject any board that doesn't match the known values. After the correct detection of soldering joints, the next checks the distance between all neighboring joints, using the previous acquired information. A distance is computed between each neighboring soldering joints, using the Euclidean distance formula, for the distance between horizontal and vertical soldering points:

$$d_x = \sqrt{(\alpha_2 - \alpha_1)^2 + (y_2 - y_1)^2} \qquad (9)$$

$$d_y = \sqrt{(x_2 - x_1)^2 + (\beta_2 - \beta_1)^2} \qquad (10)$$

were $\alpha_1 = x_1 + r_1$, $\alpha_2 = x_2 - r_2$, $\beta_1 = y_1 + r_1$ and $\beta_2 = y_2 - r_2$. x_1, x_2, y_1 and y_2 are the center points, while r_1, r_2 are the radiuses of the soldering joints. If any detected distance exceeds the accepted distance threshold value, both vertically or horizontally, then the system will reject the board.

Figure 7. Enhancement of soldering joints image; (a) inverted image, (b) result of intensity shift

After the distance calculation, the next step performs the gray level check. The darkness of the soldering joint is associated with the quality of the soldering, for instance, a lighter level represents lower soldering intensity while a darker color means that soldering intensity is high. In this respect, the image is enhanced by changing the gray level intensity, which results in making the less dense part disappearing from the image.

After increasing the intensity, the histogram of the circular area of the soldering joint is computed.

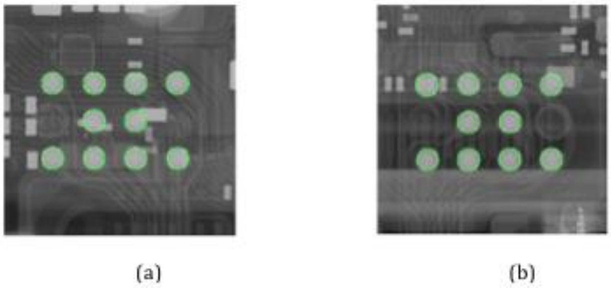

Figure 8. Detection of the soldering joints

If any detected soldering joint's histogram value is higher or lower than the accepted threshold values, then the system will consider that board as defected.

4.2. Detection of group 2 type of defects

Verification of the sub-images corresponding to this group requires the following: 1) enhancement of image; 2) detection of the circuit tracks; 3) compute the width of the tracks; 4) determine the distance between the neighboring pins.

The image was enhanced using a Gaussian filter with 3x3 kernel and sigma value of 0.5. The first step in detecting circuit's pins was the segmentation of objects of interest. As the X-ray images have many overlapping layers, it is very difficult to achieve 100% image segmentation and isolate the tracks. In the case of image 3.3 and 3.4, a cropped region is processed.

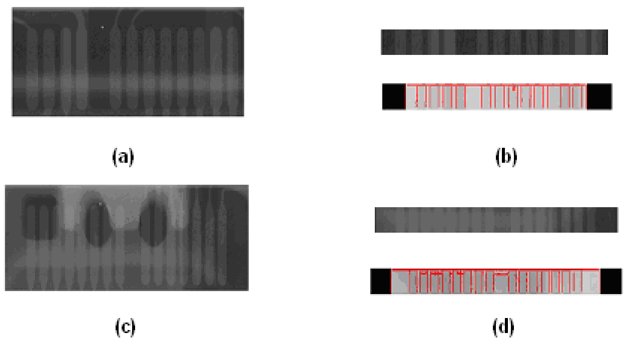

Figure 9. Region of interest processing of group 2; (a) and (c) cropped parts of image type 3.3 and 3.4; (b) and (d) shows the identification of tracks

In case of image type 3.10 and 3.11, a human segmentation was completed and the resulting masks were saved. Using this information, after segmentation, the image is then binarised. The edges were detected of every track using a fast edge detection algorithm [4], followed by a width and distance between adjacent pins estimation.

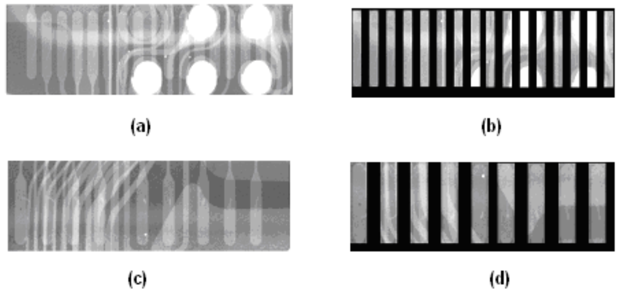

Figure 10. The processing of images type 3.10 and 3.1; (a) and (c) shows the zoomed part; (b) and (d) shows the results of human segmentation

For all the acquired images, the width and distance between adjacent pins is calculated and compared to the values of accepted thresholds. If any value does not fall within the threshold values, the board is classified as defect.

4.3. Detection of group 3 type of defects

To check the images within this group, the following steps have been completed: 1) image enhancement; 2) image segmentation; 3) checking the completeness of pins; 4) finding the soldering joints; 5) measure the size of soldering joints; 6) compute the distance between neighboring soldering joints.

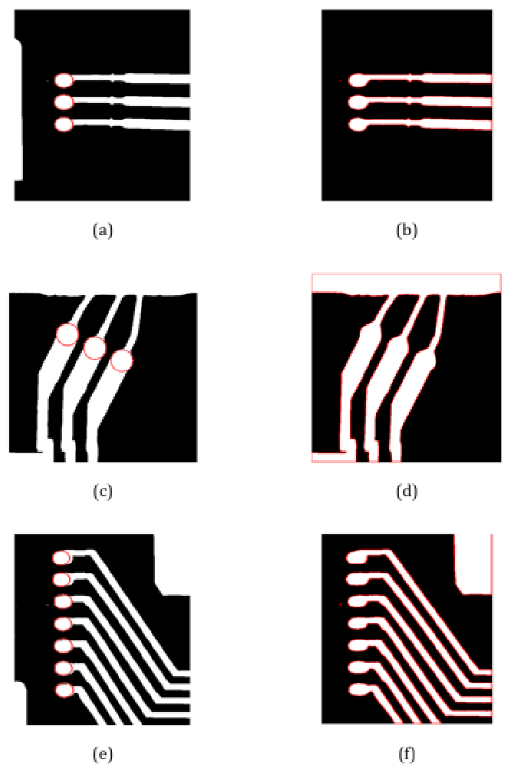

Figure 11. Images (a), (c) and (e) shows the soldering joints identification, where (b), (d) and (f) shows the detection of pins along with the soldering joints

In the case of image type 3.5, as directed by the production company, only 3 soldering joints are needed to be checked, as in the image there are around 8 soldering joints. In order to speed-up the process, a cropped image was fed to the processing block.

The X-ray image is enhanced using a Gaussian filter with 3x3 kernel and sigma value of 0.5. For the detection of soldering joints, size and intensity, the same procedure as for the image type 3.1 and 3.2 is used. If the number of soldering joints is different than the requested value or the joints are smaller or larger in size than the acceptable threshold values, or their soldering intensity is not within the range of the thresholds, then the board is consider as defect.

In the resulting images, pins and soldering joints are visible. There will be two possibilities: take the soldering joints as part of pins or subtract the soldering joints and only check the pins. Both possibilities have given nearly the same result, therefore for speed-up reasons we didn't remove the soldering joints. The eight-neighbor algorithm is used to check the completeness of the pins. Any PCB image, which does not fall within the acceptable values, will be considered as a defect board.

4.4. Detection of group 4 type of defects

In this case, the following processing steps have been completed: 1) image enhancement; 2) image segmentation in layers; 3) subtraction of layers; 4) check for breaks in pins; 5) evaluation of the distance between the pins.

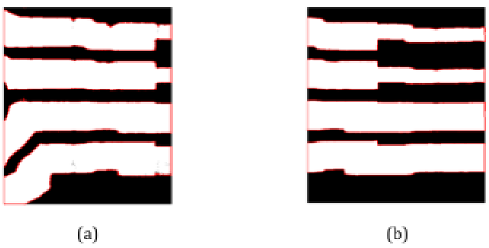

Figure 12. Group 4 defects. The segmented (a) right and (b) left part of the acquired image

The image was enhanced using a Gaussian filter, with a 3x3 kernel and 0.5 sigma value. The result was cropped in two parts and the segmentation was completed on both parts separately.

For segmentation, an assumption is made that all the images are taken under nearly the same kind of light, this assumption is logical as the images are taken by camera and light in a controlled environment and any change in light and camera might mean change of a setup. Using that assumption, segmentation is based upon the light intensity:

$$I_s = I > 2^n \tag{11}$$

where *n* in our case, varies from 11 to 13 for different images.

Equation 11 was used for the segmentation of the first part, shown in figure 12(a) with a value of *n* = 11, as the second part shown in figure 12(b) utilizes a value of *n* = 12. After obtaining both segmented images, checking the pins employs the eight-neighbor algorithm described above.

Using equation 9, the distance between the neighboring pins is computed. If the distance is more than an accepted threshold value, the board is considered as defect.

4.5. Detection of group 5 type of defects

The X-ray image is enhanced using the same Gaussian filter as above, followed by a segmentation using equation 4, with *n* = 11. A boundary box was realized around every pin, using a fast edge detection algorithm [5] modified in a way that it finds the starting and the ending point of every pin rather than trying to find every possible edge. After obtaining the dimension of boundary boxes, equation 9 is used to compute the distance between the neighboring pins. If the distance between pins is more than an accepted threshold, the board is considered as defect.

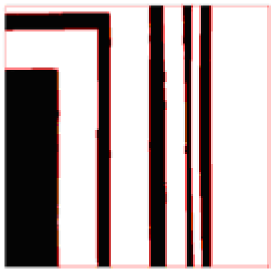

Figure 13. The result of pin identification

5. Results

At first, all the available images were processed in order to collect the results for data analysis. In the following tables, the evolution of different statistical values is presented. The first column contains the total number of images presented to the system, while the second and the third column represent how many true positive images, and respectively true negatives were fed to the system. The fourth column contains the ratio between true positive and true negative images and the fifth column contains information about the correct detection of true positive images, followed by the correct detection of true negative images by the system. The next two columns present the same information in percentage form. The last column gives the total errors made by the system in percentages. The following graph shows the correct detection of the true positive and true negative images in percentage.

Table 3. The evolution of different statistical values for the case of a defect group 1 images

Test image type 3.1								
Total Images	*True Positives (TP)*	*True Negatives (TN)*	*Ratio between TP and TN*	*Correct detection of TP*	*Correct detection of TN*	*Percentage of correct finding of TP*	*Percentage of correct finding of TN*	*Error Percentage*
50	49	1	2.0	38	0	77.6	0	24
100	95	5	5.3	75	3	78.9	60	22
200	190	10	5.3	154	7	81.1	70	19.5
400	375	25	6.7	311	18	82.9	72	17.75
800	750	50	6.7	673	39	89.7	78	11
1000	920	80	8.7	845	64	91.8	80	9.1
2000	1800	200	11.1	1675	166	93.1	83	7.95

Table 4. The evolution of different statistical values for the case of a defect group 1 images

Test image type 3.2								
Total Images	*True Positives (TP)*	*True Negatives (TN)*	*Ratio between TP and TN*	*Correct detection of TP*	*Correct detection of TN*	*Percentage of correct finding of TP*	*Percentage of correct finding of TN*	*Error Percentage*
50	49	1	2.0	40	0	81.6	0	20
100	95	5	5.3	77	4	81.1	80	19
200	190	10	5.3	160	7	84.2	70	16.5
400	375	25	6.7	320	18	85.3	72	15.5
800	750	50	6.7	680	40	90.7	80	10.0
1000	920	80	8.7	852	69	92.6	86.25	7.9
2000	1800	200	11.1	1682	175	93.4	87.5	7.15

Table 3. and 4. present the results for image type of figure 3.1 and 3.2, respectively. The results show that if more images are fed to the system, the accuracy of the system increases. It also can be observed that if comparing to true negatives, detection of true positive is done with more accuracy. The same study was performed for all the 5 group categories and results similar to the ones depicted in table 3., 4., figure 14. and 15. were obtained. In the aim of reducing the length of the paper, we have only shown the first two cases.

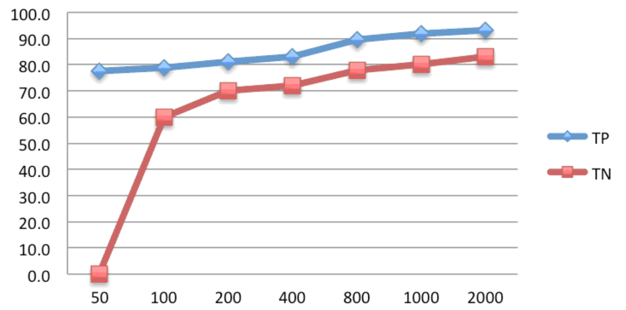

Figure 14. The evolution of true positive and true negative defect detection in percentage, for image type 3.1

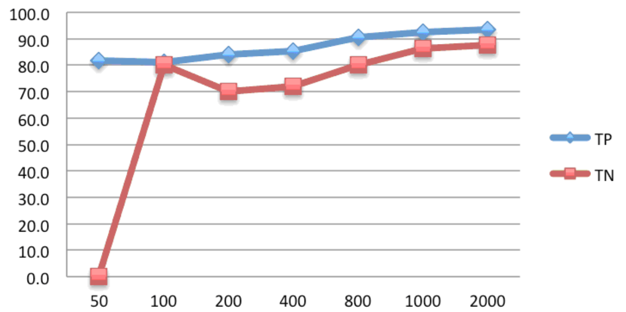

Figure 15. The evolution of true positive and true negative defect detection in percentage, for image type 3.2

The error charts have been drawn in order to follow the rate while a different number of images were presented to the system. The charts offer visual information in order to compare the errors rate of different images. As more images were presented to the system, it manages to learn and evolve. This learning and evolution happened in terms of optimization of threshold values for every single test image.

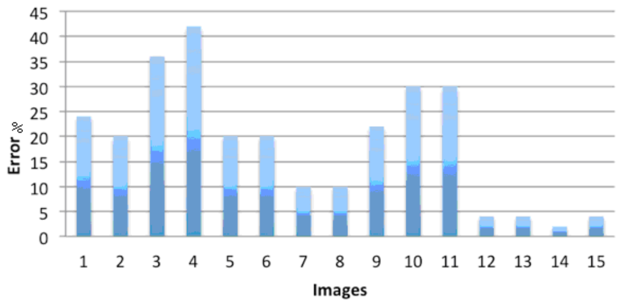

Figure 16. The error for all 15 types of test images after the presentation of 50 train images

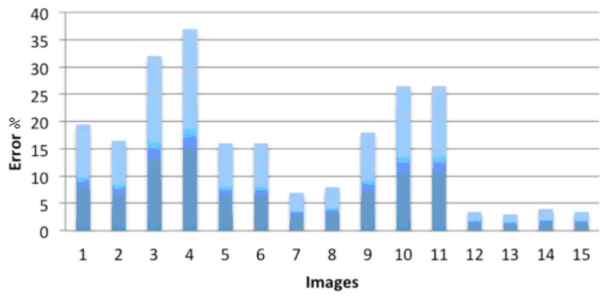

Figure 17. The error for all 15 types of test images after the presentation of 200 train images

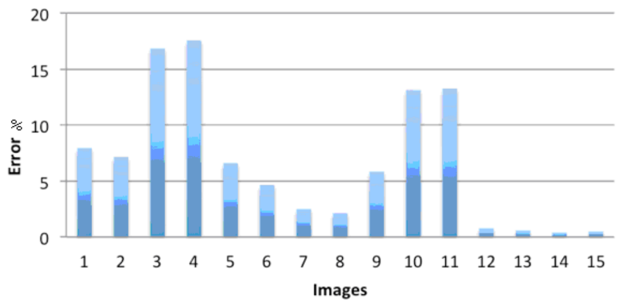

Figure 18. The error for all 15 types of test images after the presentation of 2000 train images

A set of 100 images was used for the time consuming analysis, using a MAC machine with i7 processor and 8GB of RAM. The software was developed in Matlab 2011, and for time calculation matlab's tic and toc functions were used.

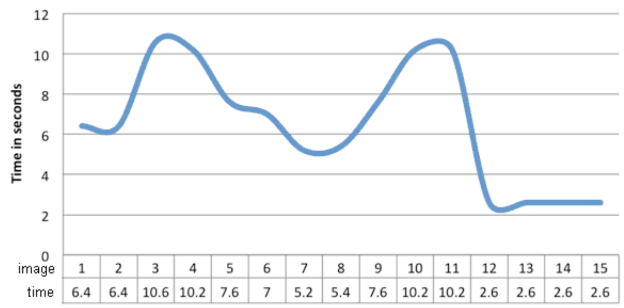

Figure 19. The processing time requested for each type of images

Figure 19. shows the average time required to perform the checking process for every type of image. The classification process took on average about 3.1 seconds. If the system is run in parallel mode, an average total amount of time of 13.7 seconds was required, while in serial mode an average 143.7 seconds was necessary. As the system doesn't need any training, the number of boards that can be checked in a day can be calculated with:

$$B_w = \frac{worktime}{t_1} \tag{12}$$

where t_1= 13.7s in parallel mode and 143.7s in serial mode. The results for parallel mode give 6307 boards per day and 601 in serial mode.

Table 5. Comparison between the existing system and the proposed system, for parallel computation

	B_w with t_1=120	B_w with parallel AVI	Boards checked in saved time	Error	Saving due to the proposed system in Euro
Week	4408	44149	39741	7505	16117.8
Month	17630	176596	158966	30021	64472.3
Year	211560	2119152	1907592	360256	773668.1

Table 5. shows the comparison between the current system and the proposed AVI system. The error column represents the total possible errors that can occur due to the usage of the AVI system. For the calculation presented, the error rate was set to 17%, as the maximum possible error found in any image according to the data presented. The last column represents financial savings, assuming the cost of a single board checking as 0.5 Euros.

6. Conclusion

A scheme of the conversion, from skilled worker based quality assurance system to an automated quality assurance system was presented. The current system was design for a specific scenario and can be called a tailor made system. The main objective was to minimize the time required for QA operations, therefore a fully automated system was proposed. The automated system takes average 13.7 seconds to complete all the tasks in parallel mode and 143.7 seconds in serial mode. The required time can decrease significantly if the same system is run on a dedicated server, in parallel with optimized code. The proposed checking processes were designed with the ability to evolve in real time, as the results have shown that their performance was improved.

References

[1] Batchelor, Bruce G., and Paul F. Whelan. *Intelligent vision systems for industry*. Springer Science & Business Media, 2012.

[2] Yu, Shiaw-Shian, Wen-Chin Cheng, and Chris SC Chiang. "Printed circuit board inspection system PI/1." *1988 Robotics Conferences*. International Society for Optics and Photonics, 1989.

[3] Janóczki, Mihály, et al. "Automatic Optical Inspection of Soldering." *Materials Science-Advanced Topics* (2013).

[4] Chen, Ssu-Han, and Der-Baau Perng. "Automatic optical inspection system for IC molding surface." *Journal of Intelligent Manufacturing* (2014): 1-12.

[5] Syed Usama Bukhari, Ioan Bondrea, Remus Brad, Augmented Reality System to Help Train New Skilled Workers for PCB Inspection, Industrial Engineering Letters, Vol. 5, No 7, pp. 1-4, 2015.

[6] Harris, Douglas H., and Frederick B. Chaney. Human factors in quality assurance. Vol. 7. John Wiley & Sons, 1969.

[7] Huang, Szu-Hao, and Ying-Cheng Pan. "Automated visual inspection in the semiconductor industry: A survey." *Computers in Industry* 66 (2015): 1-10.

[8] Mangin, Charles-Henri. "Where quality is lost on SMT boards." *Circuits Assembly* February (1991): 63-64.

[9] Kumar, Ajay. "Computer-vision-based fabric defect detection: a survey."*Industrial Electronics, IEEE Transactions on* 55.1 (2008): 348-363.

[10] Mukai, Shin. "PCB continuous line system proceeds from manufacturing to inspection." *Journal of Electronic Engineering* 29.305 (1992): 34-39.

[11] Foster, Joseph W., et al. "Automated visual inspection: a tutorial." *Computers & Industrial Engineering* 18.4 (1990): 493-504.

[12] Yu, Shiaw-Shian, Wen-Chin Cheng, and Chris SC Chiang. "Printed circuit board inspection system PI/1." *1988 Robotics Conferences*. International Society for Optics and Photonics, 1989.

[13] Bin-Nun, Emanuel. "Automatic optical inspection focuses on defects." *Electron. Packag. Prod* (1984): 82-87.

[14] Singh, Ashish, Vimal H. Nayak, and Mohammed G. Vayada. "Automatic Detection of PCB Defects." *International Journal for Scientific Research and Development* 1.6 (2014): 285-289.

[15] Putera, Siti Hazurah Indera, Syahrul Fahmi Dzafaruddin, and Maziah Mohamad. "MATLAB based defect detection and classification of printed circuit board." *Digital Information and Communication Technology and it's Applications (DICTAP), 2012 Second International Conference on*. IEEE, 2012.

[16] Londe, Prachi P., and S. A. Chavan. "Automatic PCB Defects Detection and Classification using Matlab." (2014).

[17] Kanimozhi, S., and K. Gopala Krishnan. "A review on Automatic Bare PCB Board Testing." (2013).

[18] Kumar, Ajay, and Kwok-Hung Grantham Pang. "Defect detection system for quality assurance using automated visual inspection." U.S. Patent No. 6,753,965. 22 Jun. 2004.

[19] Guh, R-S., and J. D. T. Tannock. "A neural network approach to characterize pattern parameters in process control charts." *Journal of Intelligent Manufacturing* 10.5 (1999): 449-462.

[20] Lin, Shih-Chieh, and Chia-Hsin Su. "A visual inspection system for surface mounted devices on printed circuit board." *Cybernetics and Intelligent Systems, 2006 IEEE Conference on*. IEEE, 2006.

[21] Ibrahim, Zuwairie, Noor Khafifah Khalid, and Mohamad Shukri Zainal Abidin. "An algorithm to group defects on printed circuit board for automated visual inspection." *International Journal of Simulation: Systems, Science, and Technology* 9.2 (2008): 1-10.

[22] Chin, Roland T., and Charles A. Harlow. "Automated visual inspection: A survey." *Pattern Analysis and Machine Intelligence, IEEE Transactions on* 6 (1982): 557-573.